Werk

Jahr: 1980
Kollektion: fid.geo
Signatur: 8 Z NAT 2148:48
Digitalisiert: Niedersächsische Staats- und Universitätsbibliothek Göttingen
Werk Id: PPN1015067948_0048
PURL: http://resolver.sub.uni-goettingen.de/purl?PPN1015067948_0048

LOG Id: LOG_0013
LOG Titel: Coordinated magnetic observations of morning sector auroral zone currents with triad and the scandinavian magnetometer array : a case study
LOG Typ: article

Übergeordnetes Werk

Werk Id: PPN1015067948
PURL: http://resolver.sub.uni-goettingen.de/purl?PPN1015067948
OPAC: http://opac.sub.uni-goettingen.de/DB=1/PPN?PPN=1015067948

Contact

Niedersächsische Staats- und Universitätsbibliothek Göttingen
Georg-August-Universität Göttingen
Platz der Göttinger Sieben 1
37073 Göttingen
Germany
Email: gdz@sub.uni-goettingen.de

J. Geophys. 48, 7–17, 1980

Journal of Geophysics

Coordinated Magnetic Observations of Morning Sector Auroral Zone Currents With Triad and the Scandinavian Magnetometer Array: A Case Study

H. Sulzbacher[1], W. Baumjohann[1], and T.A. Potemra[2]

[1] Institut für Geophysik, Universität Münster, Gievenbecker Weg 61, D-4400 Münster, Federal Republic of Germany

[2] Applied Physics Laboratory, Johns Hopkins University, Laurel, Maryland 20810, USA

Abstract. By using coordinated two-dimensional ground-based and satellite magnetic measurements obtained during a morning sector pass of the Triad satellite over the Scandinavian Magnetometer Array we were able to derive current densities of a large-scale westward electrojet system as well as those of a small-scale arc-associated system. The broad westward electrojet constituted a Hall current flowing in the same region where balanced field-aligned current sheets were observed. The field-aligned currents were directed downward in the north and upward in the south and were closed in the ionosphere by southward Pedersen currents. South of the maximum of the broad electrojet, in the region of grossly upward field-aligned current and near to a quiet auroral arc, another small-scale current system was found with essentially the same configuration as the electrojet system. The current densities of this arc-associated system were slightly higher or comparable to those calculated for the electrojet system.

Computation of the Σ_H/Σ_P ratio gave an indication of the latitudinal distribution of energetic particle precipitation. In contrast to the evening sector, the energetic particles precipitate in the southern half of the auroral oval, where Σ_H/Σ_P ratios of 2, and up to 4 near the auroral arc, have been found, while ratios close to 1 in the northern half indicate lower energetic electron precipitation. In addition we have also paid attention to the comparatively smaller magnetic disturbances observed by Triad perpendicular to the field-aligned current sheets and along the vertical axis. The perpendicular horizontal variation may be explained by the leakage of the toroidal magnetic field due to east-west gradients of the field-aligned sheet current density. The variations in the vertical component are due to the same source as the north-south component and can be seen because of the inclination of the field lines.

Key words: Triad satellite – Scandinavian Magnetometer Array – Morning sector auroral electrojets – Field-aligned currents – Auroral arc currents.

1. Introduction

It is a well-known fact that magnetic measurements on the earth's surface are not sufficient in order to determine the *real* three-dimensional current distributions responsible for geomagnetic disturbances. Instead, there are always various *equivalent* current systems that may explain a magnetic disturbance field configuration observed on the ground. A good example for this basic problem in the field of geomagnetism was the different way in which on one side Birkeland and Alfvén (Birkeland 1908, 1913; Alfvén 1939, 1940) and on the other hand Chapman and Vestine (Chapman 1935; Vestine and Chapman 1938) explained the main features of high-latitude magnetic variations. Birkeland and Alfvén proposed a three-dimensional ionospheric and field-aligned current system whereas Chapman and Vestine preferred a two-dimensional system confined to the ionosphere. At that time, when only ground-based magnetic observations were possible, the debate could not be settled since both current systems have equivalent ground magnetic effects (Fukushima 1969).

On the other hand, magnetic measurements still play an important rôle in the exploration of ionospheric and magnetospheric currents, because the more direct methods as, for example, the measurement of plasma parameters by means of incoherent scatter, sounding rocket or satellite experiments, also have inherent difficulties. For example, one can underestimate the field-aligned current flow by counting only particles in a limited energy range with rocket and satellite spectrometers, as described by Klumpar et al. (1976) and Evans et al. (1977). Furthermore, the 'equivalence problem' can be overcome by including measurements of additional relevant quantities like conductivity and electric fields in the analysis (see Baumjohann et al. (1980) for a broader discussion of this topic).

Another possible solution would be magnetic observations made on a three-dimensional grid. Up to now nobody has built a 'three-dimensional magnetometer array', but one magnetometer configuration which for certain magnetic disturbances may come close to this ideal case consists of the two-dimensional Scandinavian Magnetometer Array (Küppers et al. 1979) and the Triad satellite (Armstrong and Zmuda 1973). Provided that the current flows are stable during the satellite pass, the magnetic measurements along the trajectory can partially add the third dimension.

For a first case study in using coordinated Scandinavian Magnetometer Array and Triad observations for analysing auroral zone currents we have chosen a morning sector pass of the Triad satellite over a westward electrojet since here the ground magnetic fields were rather stable and indicated two-dimensionality, i.e., independency of the east-west coordinate. There have been extensive studies of ionospheric and field-aligned currents based on data from the Alaska or Alberta meridian chains of magnetometers and the geomagnetically east-west aligned component of the Triad magnetometer (e.g., Armstrong et al. 1975; Rostoker et al. 1975; Kamide and Akasofu 1976; Kamide et al. 1976b; Kamide and Rostoker 1977). As compared to these earlier studies, we have incorporated three

0340-062X/80/0048/0007/$02.20

improvements in our analysis: The first improvement is that with the array measurements we were able to show that the magnetic fields were indeed nearly two-dimensional which verified the validity of a two-dimensional analysis. The second important difference is that our analysis is quantitative instead of qualitative, as were the earlier ones. The last improvement is an additional discussion and interpretation of the comparatively small magnetic variations observed by the Triad satellite in the north-south and vertical directions.

By means of separation and subsequent upward continuation of the external part of the ground magnetic fields to ionospheric heights with a method similar to that recently applied by Mersmann et al. (1979) we were able to compare directly the latitudinal distribution of magnetic fields at 100 km (just below the ionospheric current layer) and at the Triad altitude of 800 km (above the ionosphere and in the region of field-aligned currents). Using this data set we calculated current densities for Hall, Pedersen and field-aligned currents. The high spatial resolution of our results permitted us to discuss even a small-scale structure in the westward electrojet system associated with an auroral arc. In addition, computation of the ratio between Hall and Pedersen conductivity allowed us to draw some conclusions on the latitudinal distribution of the energy of precipitating particles. Finally, we were also able to explain the magnetic observations made by Triad in the north-south and vertical directions in the framework of the whole three-dimensional current system.

2. Instrumentation and Data

On February 22, 1978, between 2237 and 2239 UT (around 0130 MLT) the Triad satellite traversed the postmidnight auroral oval over Scandinavia. Figure 1 displays the temporal variations of the geomagnetic components observed at the observatory of Kiruna, Sweden (67.8° N, 20.4° E). The magnetogram indicates that the pass occurred between two negative magnetic bays and

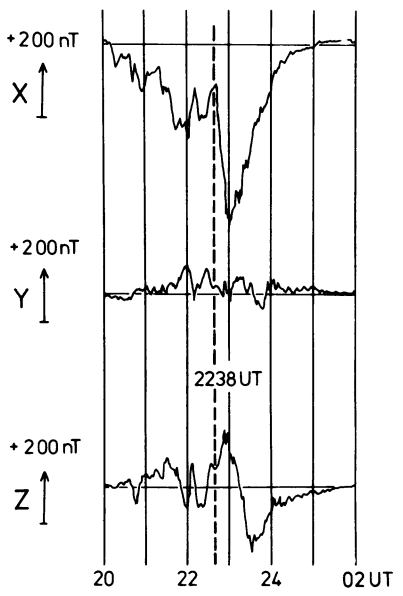

Fig. 1. Standard magnetogram from the geomagnetic observatory at Kiruna for February 22, 1978. The vertical dashed line gives the time when Triad passed approximately over Kiruna

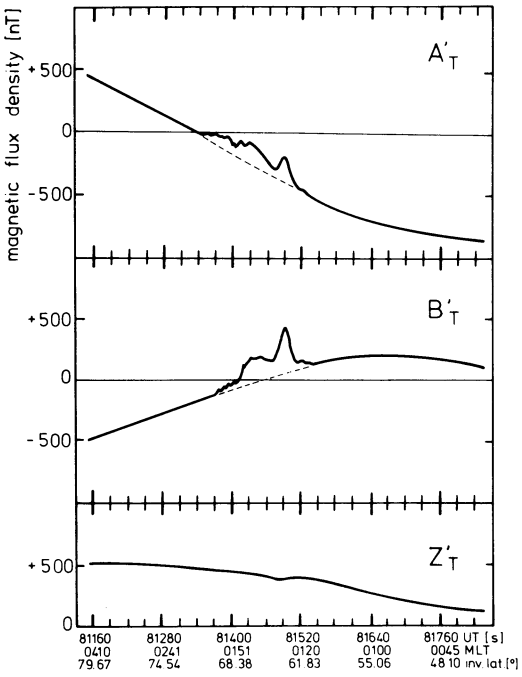

Fig. 2. Magnetic deflections along the satellite trajectory observed on February 22, 1978 around 2238 UT. The A'_T, B'_T, and Z'_T components are more commonly known as A, B, and Z components, but have been renamed to omit confusion with the Kiruna system A, B, and Z components (see Fig. 3 and text). The *dashed lines* in the A'_T and B'_T diagrams give the baseline relative to which the disturbances investigated in our analysis have been defined

during a time when the magnetic field was rather stable intermittently. This is confirmed by our other ground observations. Accordingly, all disturbances observed with the Triad magnetometer along the satellite track could be attributed to spatial variations.

A detailed description of the triaxial magnetometer onboard Triad has been given by Armstrong and Zmuda (1973). Figure 2 shows the magnetic variations observed at a rate of 2.25 samples per axis and per second during the above mentioned time interval. When passing southbound over Scandinavia the A'_T Triad magnetometer axis is directed approximately 30° west of geomagnetic north, and the B'_T axis is directed about 30° south of geomagnetic west. Accordingly, opposite to Alaskan passes, where the A'_T sensor is aligned nearly in the magnetic east-west direction, both horizontal sensors show significant variations. The Z'_T sensor shows only very weak variations. This sensor is directed vertically upwards, and is therefore not antiparallel to the main magnetic field vector.

A complete description of the Scandinavian Magnetometer Array has been given by Küppers et al. (1979). We therefore only display the locations of the magnetometers used in this study in Fig. 3, by giving the spatial distribution of 2 min averaged (2237–2239 UT) equivalent current vectors on the earth's surface (in nT). These vectors have their origin at the station where the corresponding magnetic disturbance has been observed. The 10 s averaged horizontal magnetic field vectors along the satellite track are also drawn into the same figure, with the satellite trajectory projected down to 100 km height along the magnetic field lines. The equivalent current vectors are given relative to

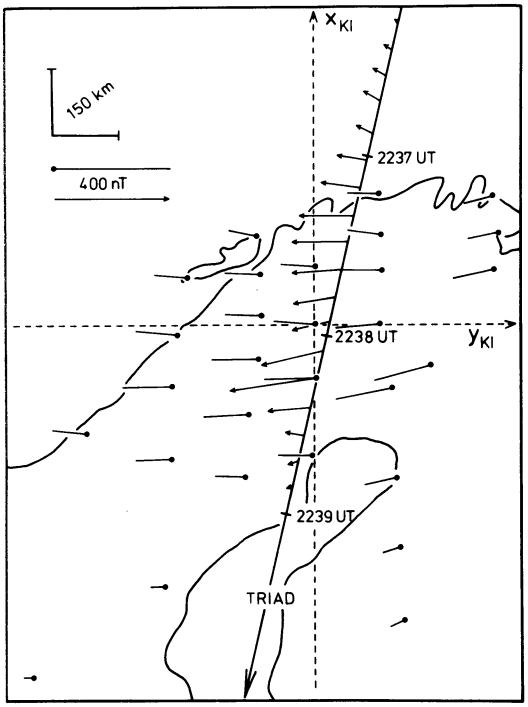

Fig. 3. Two minutes averaged equivalent current vectors on the ground and 10 s averaged horizontal magnetic disturbance vectors along the satellite track (projected down along the fieldlines to 100 km). The equivalent current vectors have their origin (*solid dot*) at the station where the corresponding magnetic disturbance has been observed. Also indicated are the axes of the Kiruna system which is explained in the text

the quiet night level, while the Triad magnetic field vectors are given relative to the baselines shown in Fig. 2. These baselines have been constructed by fitting cubic splines to the undisturbed magnetic components north of 70° and south of 60° invariant latitudes.

It can be seen that the main equivalent current flow constitutes a westward electrojet and that both equivalent current arrows and satellite magnetic fields are nearly everywhere westward directed. The constant westward direction of the equivalent current arrows indicates that the electrojet was flowing uniformly in longitude. The maximum westward magnetic field at 800 km height coincides (as projected down along the field line) with the maximum westward equivalent current arrows on the ground, but a secondary maximum can be seen in the Triad data near the northern coast of Norway. The ground-based magnetometers show no corresponding maximum of equivalent currents, but a slower decrease of current intensity north of the maximum westward current flow than south of it.

The coordinate system indicated in Fig. 3 was described by Küppers et al. (1980) and was named the Kiruna system. It is a Cartesian coordinate system obtained by a stereographic projection of the globe onto a tangential plane centered at Kiruna, Sweden. Cartesian coordinates are very suitable for analysing local ionospheric-magnetospheric current systems as done within this paper. The y_{KI} axis of the system whose origin is situated at Kiruna has been chosen as the tangent to the projection of the line $\phi_c = \phi_c\,(\mathrm{KIR}) = 64.8°$ with ϕ_c denoting the revised corrected geomagnetic latitude as given by Gustafsson (1970). The x_{KI} axis points about 12° west of geographic north at Kiruna. The horizontal components of the magnetic disturbances observed with the satellite and on the ground have been mapped into this system and have been denoted (A_T, B_T) and (A_M, B_M), respectively. The A components are aligned parallel to the x_{KI} axis and the B components parallel y_{KI}. Z_M and Z_T components and z axis are aligned perpendicular to this plane and are positive when vertically downward directed.

3. Separation and Upward Continuation of Two-Dimensional Ground Magnetic Fields

The rather constant westward direction of equivalent current arrows and Triad magnetic fields suggest that it is possible to apply methods of two-dimensional potential theory for computing the external part of the southward magnetic field distribution along the x_{KI} axis at ionospheric heights. Two-dimensionality in this respect means that all quantities are independent of one coordinate which in our case turns out to be y_{KI}.

The latter fact is illustrated by Fig. 4 where we have plotted the observed A_M and Z_M components (average values between 2237 and 2239 UT, see above) versus x_{KI}. The figure shows that there is indeed little y_{KI} dependence especially in the A_M component, while the larger scatter in the Z_M components is very probably due to local induction anomalies or coastal effects (see

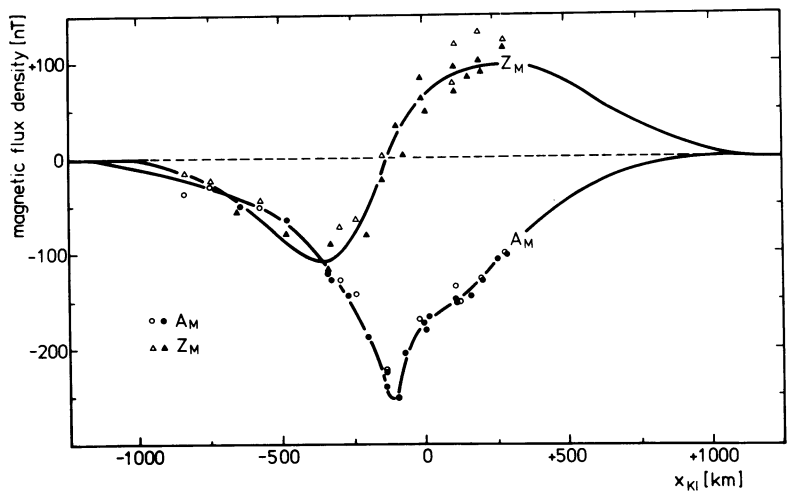

Fig. 4. Average latitude profiles of A_M and Z_M components (*solid lines*) observed on the ground. The *solid dots* and *triangles* denote A_M and Z_M field values observed at stations within $-150\,\mathrm{km} < y_{KI} < +150\,\mathrm{km}$, i.e., close to the Triad trajectory (cf. Fig. 3), while *open dots* and *triangles* denote components observed at more distant locations

Küppers et al. 1979, for a discussion of this topic). Accordingly a two-dimensional analysis can be applied to the (A_M, Z_M) components in a (x_{KI}, z) coordinate system. For that purpose we have constructed an average latitudinal profile of the observed A_M and Z_M component each along the x_{KI} axis, with an extrapolation towards zero on both sides (solid lines in Fig. 4). It should be noted that the A_M profile clearly shows the aforementioned asymmetry around the sharp peak. The Z_M profile crosses the zero level at the minimum of A_M and also shows an asymmetric distribution.

If the A_M and Z_M components are assumed to be periodic along the x_{KI} axis, with $2\pi k_0^{-1}$ defining the basic spatial wavelength (large as compared to the length of our profiles), the following Fourier expansions of the external and internal parts of these components are valid between the ionosphere and the conducting layers in the earth (in these and the following formulas we use x and y instead x_{KI} and y_{KI} for the sake of simplicity)

$$
\begin{aligned}
A_{Me}(x,z) &= -j\sum_{n=0}^{\infty} a_n\, e^{jkx-kz},\\
A_{Mi}(x,z) &= -j\sum_{n=0}^{\infty} b_n\, e^{jkx+kz},\\
Z_{Me}(x,z) &= +\sum_{n=0}^{\infty} a_n\, e^{jkx-kz},\\
Z_{Mi}(x,z) &= -\sum_{n=0}^{\infty} b_n\, e^{jkx+kz},
\end{aligned}
\tag{1}
$$

where $k = n \cdot k_0$ denotes the wavenumber and j the imaginary unit. The A_{Me} and Z_{Me} components are caused by external sources, e.g., in the ionosphere and magnetosphere, and vanish for $z \to \infty$, while the A_{Mi} and Z_{Mi} vanish for $z \to -\infty$ and are caused by internal sources, i.e., induced currents below the earth's surface ($z=0$). The observed total magnetic components on the ground are given by the superposition of the external and internal parts

$$
\begin{aligned}
A_M(x,0) &= -j\sum_{n=0}^{\infty} (a_n+b_n)\, e^{jkx},\\
Z_M(x,0) &= \sum_{n=0}^{\infty} (a_n-b_n)\, e^{jkx}.
\end{aligned}
\tag{2}
$$

A comparison of Eqs. (1) and (2) shows that $F[A_{Me}(x,0)]$, the Fourier transform of the external part of A_M at the ground, i.e., the set of coefficients $-ja_n$, can be determined by a superposition of the Fourier transforms of the observed values of $A_M(x,0)$ and $Z_M(x,0)$ according to

$$
F[A_{Me}(x,0)] = \tfrac{1}{2}(F[A_M(x,0)] + jF[Z_M(x,0)]). \tag{3}
$$

Accordingly, Fourier analysis of the observed A_M and Z_M latitudinal profiles on the ground (solid lines in Fig. 4), combination of the A_M and Z_M Fourier transforms according to Eq. (3), multiplication of the resultant Fourier coefficients with e^{+kh} (h is the assumed height of the base of the ionospheric current layer) and subsequent Fourier synthesis yields the external magnetic north-south component which is due to ionospheric and magnetospheric currents just below the ionospheric current layer. We have chosen $h = 100$ km according to the observed average height distribution of westward electrojets (Kamide and Brekke 1977).

This method is similar to that recently applied by Mersmann et al. (1979). The basic difference is that they separated external and internal parts in the spatial domain by using the Kertz operator, which is basically a Hilbert transform (Kertz 1954; Siebert and Kertz 1957; Weaver 1964), while we separated in the wavenumber domain. In order to avoid the problem of unstable solutions during continuation towards the sources (large factors e^{+kh} greatly enhance small scatter in short wavelength parts; see Mersmann et al. 1979) we have computed the Fourier spectra by a harmonic analysis with a sufficiently large spacing of $\Delta x_{KI} = 120$ km between neighbouring field values which were taken from the solid curves shown in Fig. 4. The average upward continued spectrum has then been synthesized with a 60 km spacing to be comparable with the 10 s averages of the westward B_T component observed by Triad.

In Fig. 5 we display the resultant A_{Me} profile at 100 km height together with the profile of the east-west disturbances B_T observed by Triad. The asymmetry of the A_M and Z_M profiles observed on the ground gives two clearly separated minima in the A_{Me} profile at ionospheric height. Both $A_{Me}(x_{KI}, -h)$ and $B_T(x_{KI})$ have nearly the same shape, the same small-scale structure, an almost identical amplitude (for both the minimum is -400 nT), and they both are confined to nearly the same latitudinal extent (about 1200 km). The wavy structures at the ends of

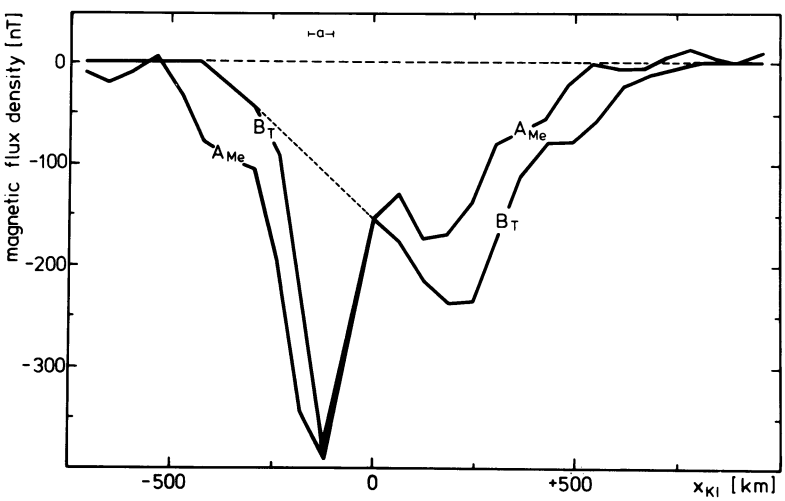

Fig. 5. Latitudinal profiles of the approximately northward external magnetic horizontal component A_{Me} at the height of 100 km (just below the assumed ionospheric current layer) and of the approximately eastward horizontal disturbance B_T observed by Triad and projected down to 100 km along the fieldlines. The A_{Me} and B_T curves can be regarded as giving westward and southward ionospheric height-integrated current density if one substitutes 100 nT by 160 mAm^{-1} for A_{Me} or 100 nT by 80 mAm^{-1} for B_T, respectively. The *horizontal dashed line* gives the zero-level, the other dashed line in the region of the small-scale structure gives the approximate magnetic flux density B_T associated with the large-scale electrojet system in this area and the bar around the small 'a' denotes the approximate position of the observed auroral arc (see text)

the A_{Me} profile belong to a spatial wavelength of 240 km, i.e., the smallest wavelength resolved in our analysis, and are very probably related to the above mentioned instability problem. The factor e^{+kh} amounts to about 15 for this wavelength, and accordingly the observed amplitude of ± 15 nT of this wavelength at $h=100$ km seems to be due to height-continued errors in A and Z that are of the order of 1 nT at ground.

4. Ionospheric and Field-Aligned Currents and the Hall to Pedersen Conductivity Ratio

For a two-dimensional situation like the present one we can relate the magnetic field distributions displayed in Fig. 5 to the *real* (not merely *equivalent*) auroral zone current system in the following way:

As Boström (1964) first clearly pointed out this system (if two-dimensional and if confined to the auroral latitudes) consists of the electrojet whose magnetic field is observed on the ground, and of meridional currents that are field-aligned above the ionosphere and are closed within the lower ionosphere (and in the magnetosphere). The meridional currents possess a toroidal magnetic field that may be parallel or antiparallel to the electrojet and that is unobservable on the ground.

Since in our case the vertical thickness of the electrojet, that flows in the negative y direction is small as compared to its latitudinal extent, its large-scale features may be described by a surface current density J_y (negative in our case). This quantity is related to the height-continued northward magnetic flux density according to

$$J_y(x)=\frac{2}{\mu_0} A_{Me}(x, -h) \tag{4}$$

if h is the height of the base of the electrojet layer (note that z denotes depth). Accordingly, the curve denoted by A_{Me} in Fig. 5 gives directly the electrojet height-integrated current density J_y if 100 nT are replaced by 160 mAm^{-1}. The maximum westward current density is 620 mAm^{-1} for the southern and 280 mAm^{-1} for the northern peak of the J_y distribution. Between these two extrema the surface current density decreases to about 210 mAm^{-1}, and the total current is approximately $2.4 \cdot 10^5$ A.

The magnetic component B_T as observed by the Triad satellite (Fig. 5) must be interpreted as the toroidal magnetic flux density generated by the poloidal (meridional) current system, as it has been done for similar disturbances since the first analyses of Triad data (e.g. Armstrong and Zmuda 1970; Zmuda and Armstrong 1974). This system may be described by a spatial field-aligned current density $j_{\parallel}(x)$ (positive if parallel to the earth's magnetic field) above the ionospheric current layer, and by a surface current density $J_x(x)$ that connects the field-aligned currents within the ionosphere. Because B_T is zero outside this current system we get from Maxwell's first equation

$$j_{\parallel}(x)=\frac{1}{\mu_0}\frac{dB_T}{dx}. \tag{5}$$

Current continuity within the poloidal system may be expressed by

$$\frac{dJ_x}{dx}=j_{\parallel}(x). \tag{6}$$

The combination of these two equations yields

$$J_x(x)=\frac{1}{\mu_0} B_T(x). \tag{7}$$

This equation shows that the second curve in Fig. 5 may be interpreted as the height-integrated density of the northward current (negative, i.e., southward in this case) in the electrojet region if 100 nT are replaced by 80 mAm^{-1}. Accordingly, we recognize a maximum southward current density of 310 mAm^{-1}, about 190 mAm^{-1} for the northern secondary extremum, and 120 mAm^{-1} in between.

The field-aligned current density has been calculated by differentiating the B_T profile (Fig. 5) according to Eq. (5). The result is displayed in the upper part of Fig. 6. The $j_{\parallel}(x)$ curve shows relatively pronounced structure that will be discussed below. The maximum current densities are 2.5 μAm^{-2} with upward and 1.5 μAm^{-2} with downward flow. The total field-aligned surface current density is 370 mAm^{-1} for both up- and downward flowing current.

Since the large-scale field-aligned currents have a magnetospheric source (e.g. Boström 1975; Rostoker and Boström 1976) the associated ionospheric electric field must be southward directed along the x_{KI} axis for the given gross pattern of upward field-aligned current flow in the south and downward in the north. Accordingly, we can interpret $J_x=\Sigma_P E_x$ as Pedersen and $J_y=\Sigma_H E_x$ as Hall current and get from Eqs. (4) and (7)

$$A_{Me}(x, -h)=\frac{1}{2}\cdot\frac{\Sigma_H}{\Sigma_P}(x)\cdot B_T(x). \tag{8}$$

The latitudinal profile of the ratio Σ_H/Σ_P which results from the profiles of A_{Me} and B_T (Fig. 5) according to this relation is given in the lower panel of Fig. 6. It shows a decrease with increasing latitude from values close to 4 near the southern boundary of the current system and in the region of intense upward field-aligned current flow to values close to 1 in the north where a broad region of downward field-aligned current is observed.

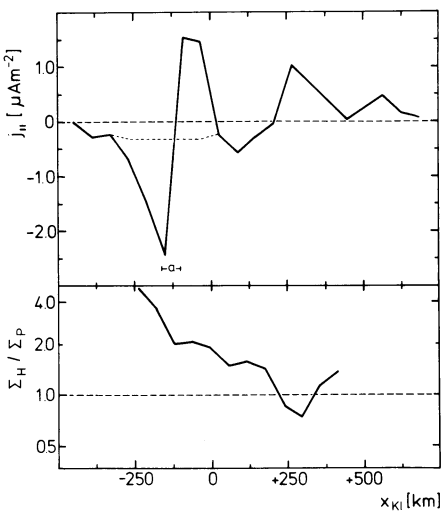

Fig. 6. The upper diagram displays the latitudinal distribution of field-aligned current density calculated by differentiating the B_T profile given in Fig. 5. Positive values denote downward currents. *Dashed line* and bar around '*a*' have the same notation as in Fig. 5. The lower panel gives the derived (cf. text) latitudinal profile of the ratio between Hall and Pedersen conductivity on a logarithmic scale

5. Magnetic Variations in the North-South and Vertical Component at Triad Altitude

In the previous sections we were concerned with the strong magnetic variations observed by Triad in the B_T (approximately geomagnetic east-west) direction and related to the meridional current system of balanced field-aligned currents and Pedersen currents. In this section we will try to interpret the comparatively smaller variations in the A_T component (approximately geomagnetic north-south; maximum amplitude about 50 nT) and the even smaller ones in the Z_T component (vertically downward; maximum amplitude about 20 nT). One possible source of magnetic variations in the A_T and Z_T components at 800 km altitude is the magnetic field associated with the electrojet. We have calculated this contribution from $J_y(x)$ as given by the curve $A_{Me}(x)$ in Fig. 5 in combination with Eq. (4). The result is given by the curves A_I and Z_I in the upper part of Fig. 7. One can see that they are changing only slowly with latitude and that they have maximum amplitudes of 50 and 20 nT for A_I and Z_I, respectively. Magnetic fields of more distant sources like the ring current should change even more slowly and may hardly be distinguishable from the quiet level. If we subtract A_I and Z_I from A_T and Z_T, respectively, we should get the residual magnetic disturbances due to probably more local sources. Since A_I and Z_I have a very gradual slope south of 60° and north of 70° invariant latitude, i.e., in the regions where we have fitted the cubic splines to construct the baseline, no decision can be made between these variations and the well-known slow variations due to the spacecraft attitude uncertainty. Accordingly, we have here first subtracted the fields of ionospheric origin and then constructed a new baseline by fitting cubic splines to the northern and southern 'undisturbed' region. The results are given in the lower part of Fig. 7 and the variations indeed reflect a quite local character.

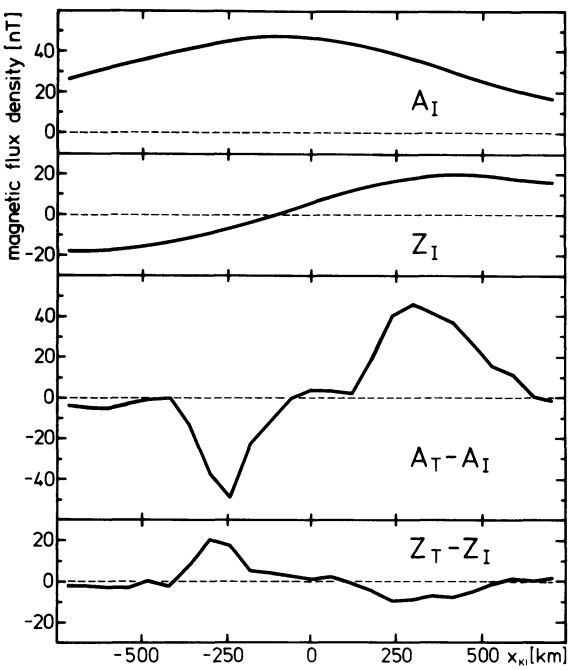

Fig. 7. The two upper panels display the magnetic flux density of the ionospheric westward electrojet (cf. Fig. 5) at a Triad altitude. The two lower panels give the magnetic disturbances observed by Triad at 800 km altitude in the northsouth and vertical component after subtraction of the above-mentioned fields of ionospheric origin

The (A_T-A_I) variations show an almost antisymmetric shape with respect to $x_{KI}\approx 0$. If one projects this location along the magnetic field lines down to 100 km altitude in order to compare it with the location where the large-scale field-aligned currents change their direction as given in the upper part of Fig. 6 (around $x_{KI}=200$ km), one finds that both locations approximately coincide. One also finds that the northern maximum (A_T-A_I) is located at the northern edge of the field-aligned region and that the southern minimum is close to the southern edge. Both these facts hint to the explanation that the (A_T-A_I) magnetic variations constitute a leakage of toroidal magnetic flux $\int B_T$ due to a westward decrease in the field-aligned current intensity. This decrease is consistent with a slight decrease of the westward electrojet in the same direction which can be noted when carefully examining Fig. 3.

The actual leakage magnetic flux density depends on both the gradient of the westward decrease and on the longitudinal location with respect to the central meridian and the western termination of the electrojet. With the data set available we cannot determine these parameters, but we have calculated the A_T component in 800 km altitude by assuming that the Pedersen-field-aligned current system given in Figs. 5 and 6 decreases linearly by 10% per 100 km in the westward direction and that the western termination was 1000 km and the central meridian 2000 km apart. The resultant curve is displayed in Fig. 8 and one can see that there is a reasonable agreement with the observed (A_T-A_I) curve of Fig. 7 regarding shape, zero-crossover, location of the extrema, and amplitude in the central region between the two arrows.

The observed (A_T-A_I) profile cannot show the very gradual increase and decrease of the calculated A_T south and north of the locations indicated by the arrows, since these are the regions

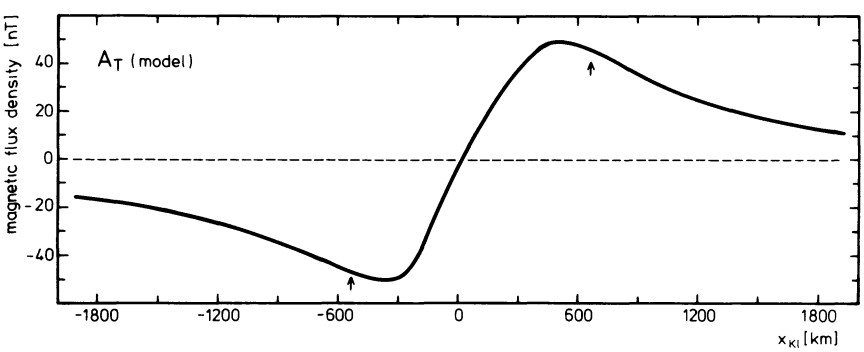

Fig. 8. Calculated northward component of magnetic flux density due to a leakage of the toroidal magnetic flux (the model current system is explained in the text). Outside the region between the *two arrows* cubic splines have been fitted to the observed data for baseline determination and no agreement between calculated and observed A_T components (Fig. 7) can be expected

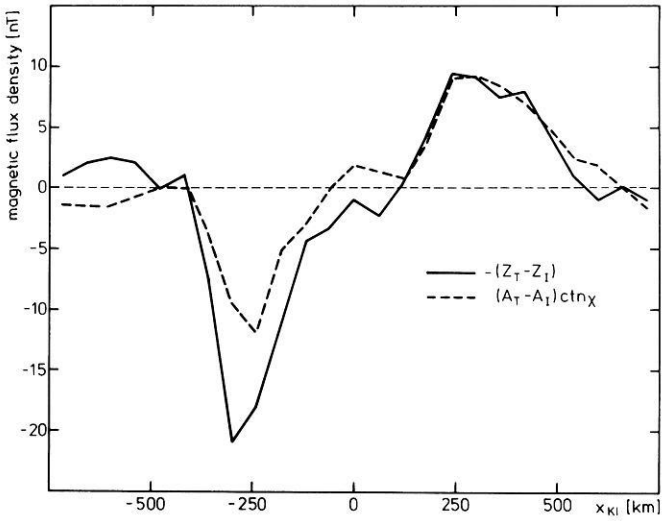

Fig. 9. Comparison of the two quantities related in Eq. (9) (χ denotes the inclination of the earth's magnetic field)

where cubic splines have been fitted to the variations observed by Triad for the baseline determination and consequently the (A_T-A_I) curve must be close to this baseline. We should also note that a westward decrease of 10% per 100 km is about twice as much as the westward decrease of the southward magnetic field observed on the ground, but we feel that our calculations give at least good evidence that the observed (A_T-A_I) variations are due to the leakage to toroidal magnetic flux.

If the Triad Z sensor would be aligned along the magnetic field direction one would expect to observe no effect of field-aligned currents in this sensor. But the sensor is actually aligned gravitationally and therefore the following relation holds (with $\chi(x)$ denoting the latitude dependent inclination of the fieldlines as given by geomagnetic charts):

$$-[Z_T(x)-Z_I(x)]=[A_T(x)-A_I(x)]\ \mathrm{ctn}\ \chi(x). \tag{9}$$

We have calculated the above two quantities and display them in Fig. 9. It can be seen that both curves agree rather well and it can therefore be assumed that the (Z_T-Z_I) variations are due to the same sources as the (A_T-A_I) variations, i.e., very probably due to the leakage of toroidal magnetic flux.

6. Discussion

Our analysis has provided results for the distribution of ionospheric Hall and Pedersen currents and field-aligned currents associated with a westward electrojet in the morning sector. The large-scale features of such current systems are already rather well known and generally in agreement with our results. Small-scale structures in the latitudinal current density distribution are still a much debated topic (Kamide 1979) and the relationship of the sharp southern peak in ionospheric current density and the intense field-aligned current sheets with an auroral arc will be discussed as the second topic. Another important result is the latitudinal dependence of the conductivity ratio, and from this we will draw some conclusions about the particle precipitation in the morning sector during the present event.

Large-Scale Currents

The electrojet constitutes a westward Hall current of about $2.4\cdot10^5$ A flowing in nearly exactly the same region where grossly balanced field-aligned current sheets of 370 mAm^{-1} are observed flowing downward in the north and upward in the south. These currents are linked in the ionosphere by southward Pedersen currents, and the toroidal magnetic field caused by this meridional current system was observed by Triad above the ionosphere and was of the order of 200–400 nT. In contrast, the meridional magnetic field of the electrojet was about 30–50 nT at the Triad altitude.

The values given above are within the range found in earlier studies with the Chatanika radar and the Triad satellite for the same local time sector (e.g. Brekke et al. 1974; Kamide and Brekke 1975; Iijima and Potemra 1976, 1978; Horwitz et al. 1978a, b; Kamide and Horwitz 1978). Also our observation that balanced field-aligned currents close along one meridian is in agreement with the statistical field-aligned current flow pattern given by other authors (Yasuhara et al. 1975; Sugiura and Potemra 1976; Iijima and Potemra 1976, 1978; Hughes and Rostoker 1977), who all note balanced field-aligned currents during 2 to 4 h around magnetic midnight.

We should note that our assumption of a purely meridional southward directed ionospheric electric field caused by the balanced field-aligned currents (and consequently the westward current to be a pure Hall current) is not without contradiction. For example Hughes and Rostoker (1977, 1979), using observations of westward electric fields around midnight by Mozer and Lucht (1974), proposed that the quiet time westward electrojet in the 22–02 MLT sector is mainly a Pedersen current while the Hall current is directed more northward. After examining a great amount of published electric field patterns (Heppner 1973, 1977; Holzworth et al. 1977; Horwitz et al. 1978a, b; Maynard 1974; Wedde et al. 1977), we have found that westward electric fields are confined mostly to the Harang-discontinuity region (where indeed northward Hall currents may be found; e.g. Kamide and Horwitz 1978; Baumjohann 1979; Baumjohann et al. 1980) in the late evening sector. Furthermore southward directed fields appear to predominate in the postmidnight sector in support of our earlier assumptions. This apparent contradiction may be resolved by the fact that Hughes and Rostoker (1977, 1979) discussed the quiet time current configuration and used quiet time electric field data while our data and most of the above cited electric field patterns are representative for more disturbed times, when the westward Pedersen current is concentrated behind the surge in the evening sector (Rostoker and Hughes 1979).

Therefore we suggest that during disturbed times the zonal westward closure current of the net field-aligned currents around magnetic midnight (Kamide et al. 1976b, c) is the Hall current whose magnetic signatures have been observed on the ground. This closure is in agreement with a model already proposed by Heppner et al. (1971a, b), and has been verified recently by Baumjohann et al. (1980) for the eastward electrojet in the dusk sector by comparing two-dimensional distributions of ionospheric electric and ground magnetic fields.

Small-Scale Current System Associated With an Auroral Arc

Mersmann et al. (1979) have found an electrojet current density that was not a smooth latitudinal distribution from their study

of an eastward electrojet with essentially the same method as applied here. In their case a small decrease in current density was found, and evidence was given that this decrease was possibly due to a local westward current inside an auroral arc. The existence of this arc could not be verified due to cloudiness and some ambiguity remained. In our case a similar structure is found both in the ionospheric and field-aligned current densities, but it is much stronger in amplitude, and is of a greater spatial wavelength (about 500 km). Again the weather in Scandinavia was rather cloudy but one of the Scandinavian all-sky-cameras produced analysable data. This camera was located at Hankasalmi in southern Finland and during the time of the Triad pass a rather stable quiet arc was seen near the northern horizon of the camera. This arc was located approximately between $x_{KI} = -160$ and -100 km (H.J. Opgenoorth private communication, 1979), which means in the region where we observed intense upward field-aligned current and strong westward ionospheric current flow (cf. Figs. 5 and 6).

Accordingly, we interpret the peaks in the observed A_{Me} and B_T curves (Fig. 5) at $x_{KI} = -120$ km as enhanced westward Hall and southward Pedersen current flow between a pair of relatively thin sheets (each about 100 km wide) of intense field-aligned currents (cf. Fig. 6 upper panel) that is associated with the observed auroral arc. The center of this system is situated about 300 km south of the secondary peaks which now may be contributed to the maximum of a broad westward electrojet current density distribution. Of the total 620 mAm^{-1} Hall current density inside or near the arc, about 450 mAm^{-1} may be attributed solely to the small-scale arc system. The arc-associated westward Hall current density is therefore greater than the maximum current density of the broad westward electrojet (270 mAm^{-1}), and the total arc-associated Hall current contributes about 20% to the total westward current. Of the maximum southward Pedersen current density of 310 mAm^{-1} about 220 mAm^{-1} may be arc-associated and are therefore of about the same magnitude as the current density near the maximum of the westward electrojet. The maximum field-aligned current densities (cf. Fig. 6, upper part) can be nearly solely attributed to the arc and we get 2 μAm^{-2} associated with the arc compared with a maximum of 1 μAm^{-2} associated with the main electrojet. In terms of sheet current densities, this means that a current of about 200 mAm^{-1} flows downward to the north of the arc and flows upward above or south of the arc. This field-aligned current closes via the southward Pedersen currents. Compared to the electrojet-associated field-aligned current, whose sheet current densities may be estimated to be also about 200 mAm^{-1}, the total arc-associated vertical currents have the same magnitude.

It should be noted that the current densities given are more minimum current densities for the arc system, since the latitudinal resolution of our analysis is restricted to spatial wavelength greater than 200 km. Auroral arcs and most probably also the associated current systems are much smaller (e.g. Davis 1978) and our data may display smoother curves and lower peaks than were actually there.

We have also compared our observations with results of rather rare earlier studies on morning sector auroral arcs. Kamide and Rostoker (1977) noted that discrete arcs in the morning sector are found in the region of intense upward field-aligned currents in the southern half of the westward electrojet. Beaujardiere et al. (1977) found, by means of incoherent scatter observations, an arc-associated enhancement of the westward current flow of about 160 mAm^{-1}. Because of their fine resolution rocket-borne experiments are best suited to study phenomena associated with auroral arcs. But to the best of our knowledge, only one rocket flight into postmidnight aurora has been made (Sesiano and Cloutier 1976). Since this rocket was flown through a highly structured multiple arc system the results are hardly comparable with ours. The field-aligned sheet current densities determined in our study are within the range (160 to 1200 mAm^{-1}) obtained from the Rice University rocket flights into auroral arcs in the premidnight sector (Anderson and Vondrak 1975).

We should note once more that our interpretation of the westward current as a Hall current, and the southward current as a Pedersen current is based on the assumption that the field-aligned currents are driven by a magnetospheric source with the ionosphere acting as a load. As described earlier, this mechanism is commonly accepted for the large-scale currents, but it is still a matter of debate if the field-aligned current pairs associated with auroral arcs are driven by the magnetosphere (e.g. Mallinckrodt and Carlson 1978) or by a polarization electric field in the ionosphere (e.g. Carlson and Kelley 1977). The second model implies an ambient zonal westward electric field which, as described earlier, is rarely observed in this MLT sector. Furthermore the non-existence of this electric field can be concluded from the rather stable location of the auroral arc (arcs drift southward under $E \times B$ motion of a westward field; see for example Kelley et al. 1971). Therefore we tend to believe that a magnetospheric source can indeed be assumed, but this question can only be decided by simultaneous electric field measurements and we hope that a future study incorporating Triad, the Scandinavian Magnetometer Array, and the STARE-radars (Greenwald et al. 1978) will help in this respect.

Hall to Pedersen Conductivity Ratio

South of $x_{KI} = 0$ km the Σ_H/Σ_P ratio varies between 2 and 4 and is within the range given by Brekke et al. (1974) based on their Chatanika radar observations. North of $x_{KI} = 0$ this ratio reduces to values around and slightly below 1, and is therefore smaller than the minimum value given by Brekke et al. (1974). But Evans et al. (1977), who computed ionospheric conductivities based on auroral electron data obtained during a sounding rocket flight, determined values between 0.8 and 1.4. Both groups used a different atmospheric model and the difference in the ratios found may very probably be attributed to uncertainties in these models, while our calculations are free from these ambiguities.

The ratio between the two conductivities allows some conclusions on the energy of precipitating particles, since energetic auroral electrons penetrating the atmosphere reach different altitude levels depending on their energy (Rees 1963). Experimental evidence for this can be found for example in Brekke et al. (1974) and Evans et al. (1977) who both noted that maximum enhancements of the Σ_H/Σ_P ratio are found to be coincident with energetic particle precipitation.

For our case this means that particles with higher energies precipitate in the southern third of the westward electrojet region, where the most intense Hall and upward field-aligned current densities and the auroral arc have been found. The average energy of the precipitating particles gradually decreases towards north, where the field-aligned currents flow downward. This latitudinal distribution of particle precipitation is oppositely to that in the evening sector (see, for example, Lui et al. 1977) but agrees with other results found in the morning sector

by direct measurements with the Isis (McDiarmid et al. 1975; Klumpar et al. 1976) and Injun (Frank and Ackerson 1971) satellites, by monochromatic all-sky observations (Mende and Eather 1976) and by studying the relative location of discrete aurora in the electrojet region (Kamide et al. 1976b; Kamide and Rostoker 1977).

7. Summary and Conclusions

In the present paper, for the case of a morning sector pass, we have demonstrated the usefulness of coordinated two-dimensional ground-based and Triad satellite magnetic observations. We have shown that, for the two-dimensional case studied, it is possible to derive quantitatively the real ionospheric-field-aligned current system and the latitudinal distribution of the Σ_H/Σ_P ratio and that it is possible to explain also variations observed by Triad in the north-south and vertical component. This has been done by using only two very basic and well accepted assumptions: that the balanced field-aligned currents are of magnetospheric origin thereby causing a purely southward electric field, and that the altitude of the ionospheric current layer is 100 km.

For the event which we investigated the more detailed results include the following:

1. A broad westward electrojet (about 1200 km wide) was observed at about 0130 MLT. It constituted a Hall current of about $2.4 \cdot 10^5$ A flowing in the same region where balanced upward and downward flowing field-aligned current sheets of about 200 mAm^{-1} were observed. These currents where closed in the auroral ionosphere along the same meridian by southward Pedersen currents of about the same maximum current density as the field-aligned currents.

2. South of the maximum of the broad electrojet and near the location of a quiet auroral arc another latitudinally small but very intense peak in the ionospheric current density was observed. This small-scale arc-associated current system had essentially the same configuration as the large-scale electrojet system. The about 250 km wide westward Hall current had a maximum density of 450 mAm^{-1}, greater than the maximum current density of the main electrojet, and contributed 20% of the total westward current. The field-aligned currents flew downward in the north and upward over or south of the arc and their maximum current densities of about 2 μAm^{-2} were twice as high as those of the electrojet associated pair. The total field-aligned current flow was closed by southward Pedersen currents of 220 mAm^{-1}.

3. While we found Σ_H/Σ_P ratios close to 1 in the northern half of the westward electrojet and in the region of downward field-aligned currents, this ratio increased to values between 2 and 4 in the southern half with the highest values near the location of the auroral arc and the intense upward field-aligned currents. Relating these ratios to the energy of precipitating particles we have concluded that in contrast to the evening sector energetic particles precipitate in the southern half of the auroral oval (as defined by the electrojet borders) where the discrete arc has been observed. Lower energetic particle precipitation appears to occur in the northern half.

4. The disturbances observed by the geomagnetic northsouth component of the Triad magnetometer (perpendicular to the field-aligned current sheets) may be explained by a leakage of the toroidal magnetic flux due to a probable decrease of the field-aligned current intensity in the westward direction. Due to the inclination of the earth's magnetic field these variations can also be seen in the gravitationally aligned vertical component.

It should be mentioned, that the present conclusions are derived on the basis of only one case studied. Future work has to show if the conclusions may be generalized.

Acknowledgements. We are greatly indebted to those past and present members of the magnetometer group at the University of Münster, who were involved in collecting the magnetic data. The magnetic observations were performed in cooperation with the Royal Institute of Technology at Stockholm, the Finnish Meteorological Institute at Helsinki, the University at Tromsö, the University of Bergen, the Geophysical Observatory Sodankylä of the Finnish Academy of Science and Letters, the Kiruna Geophysical Institute, the University of Oulu, and the Aarhus University. To these institutions our sincere thanks are due for permanent support. Invaluable assistance in the TRIAD data collection and processing was provided by S. Favin, J. Du Brul, and J. Nearvy, and the entire project was made possible by the Space Department of APL/JHU. We also wish to thank H.J. Opgenoorth for information on the auroral condition during the Triad pass and Ch. Sucksdorff and G. Gustafsson for additional magnetic data. We also thank G. Gustafsson and the Kiruna Geophysical Institute for assistance in the acquisition of the Triad data. This work has been supported financially by the Deutsche Forschungsgemeinschaft, the National Science Foundation, and the Office of Naval Research. We are grateful to Y. Kamide and G. Rostoker for their instructive referees' comments.

References

Alfvén, H.: A theory of magnetic storms and of the aurorae I. R. Swedish Acad. Sci., Proc. 3 Ser.: **18**, No. 3, 1939

Alfvén, H.: A theory of magnetic storms and of the aurorae II and III. R. Swedish Acad. Sci., Proc. 3 Ser.: **18**, No. 9, 1940

Anderson, H.R., Vondrak, R.R.: Observations of Birkeland currents at auroral latitudes. Rev. Geophys. Space Phys. **13**, 243–262, 1975

Armstrong, J.C., Akasofu, S.-I., Rostoker, G.: A comparison of satellite observations of Birkeland currents with ground observations of visible aurora and ionospheric currents. J. Geophys. Res. **80**, 575–586, 1975

Armstrong, J.C., Zmuda, A.J.: Field-aligned current at 1100 km in the auroral region measured by satellite. J. Geophys. Res. **75**, 7122–7127, 1970

Armstrong, J.C., Zmuda, A.J.: Triaxial magnetic measurements of field-aligned currents at 800 km in the auroral region: initial results. J. Geophys. Res. **78**, 6802–6807, 1973

Baumjohann, W.: Spatially inhomogeneous current configurations as seen by the Scandinavian Magnetometer Array. In: Proceedings of the International Workshop on Selected Topics of Magnetospheric Physics, Japanese IMS Committee, ed., pp. 35–40, Tokyo, 1979

Baumjohann, W., Untiedt, J., Greenwald, R.A.: Joint two-dimensional observations of ground magnetic and ionospheric electric fields associated with auroral zone currents. 1. Three-dimensional current flows associated with a substorm-intensified eastward electrojet. J. Geophys. Res. in press, 1980

Beaujardiere, O. de la, Vondrak, R., Baron, M.: Radar observations of electric fields and currents associated with auroral arcs. J. Geophys. Res. **82**, 5051–5062, 1977

Birkeland, K.: The Norwegian Aurora Polaris expedition, 1902–1903, Vol. 1: On the cause of magnetic storms and the origin of terrestrial magnetism, sect. 1. Christiania: H. Aschehoug 1908

Birkeland, K.: The Norwegian Aurora Polaris expedition 1902–1903, Vol. 1: On the cause of magnetic storms and the origin of terrestrial magnetism, sect. 2. Christiania: H. Aschehoug 1913

Boström, R.: A model of the auroral electrojets. J. Geophys. Res. **69**, 4983–5000, 1964

Boström, R.: Mechanisms for driving Birkeland currents. In: Physics of the hot plasma in the magnetosphere, B. Hultqvist, L. Stenflo, eds.: pp. 341–351. New York: Plenum Press 1975

Brekke, A., Doupnik, J.R., Banks, P.M.: Incoherent scatter measurements of *E* region conductivities and currents in the auroral zone. J. Geophys. Res. **79**, 3773–3790, 1974

Carlson, C.W., Kelley, M.C.: Observation and interpretation of particle and electric field measurements inside and adjacent to an active auroral arc. J. Geophys. Res. **82**, 2349–2360, 1977

Chapman, S.: The electric current system of magnetic storm. Terr. Magn. Atmos. Electr. **40**, 349–370, 1935

Davis, T.N.: Observed characteristics of auroral forms. Space Sci. Rev. **22**, 77–113, 1978

Evans, D.S., Maynard, N.C., Trøim, J., Jacobsen, T., Egeland, A.: Auroral vector electric field and particle comparisons. 2. Electrodynamics of an arc. J. Geophys. Res. **82**, 2235–2249, 1977

Frank, L.A., Ackerson, K.L.: Observations of charged particle precipitation into the auroral zone. J. Geophys. Res. **76**, 3612–3643, 1971

Fukushima, N.: Equivalence in ground geomagnetic effect of Chapman-Vestine's and Birkeland-Alfvén's electric current systems for polar magnetic storms. Rep. Ionos. Space Res. Jap. **23**, 219–227, 1969

Greenwald, R.A., Weiss, W., Nielsen, E., Thomson, N.R.: STARE: A new radar auroral backscatter experiment in northern Scandinavia. Radio Sci. **13**, 1021–1039, 1978

Gustafsson, G.: A revised corrected geomagnetic coordinate system. Ark. Geofys. **5**, 595–617, 1970

Heppner, J.P.: High latitude electric fields and the modulations related to interplanetary magnetic field parameters. Radio Sci. **8**, 933–948, 1973

Heppner, J.P.: Empirical models of high-latitude electric fields. J. Geophys. Res. **82**, 1115–1125, 1977

Heppner, J.P., Stolarik, J.D., Wescott, E.M.: Electric-field measurements and the identification of currents causing magnetic disturbances in the polar cap. J. Geophys. Res. **76**, 6028–6053, 1971a

Heppner, J.P., Stolarik, J.D., Wescott, E.M.: Field aligned continuity of Hall current electrojets and other consequences of density gradients in the auroral ionosphere. In: The radiating atmosphere, B.M. McCormac, ed.: pp. 407–426. Dordrecht: D. Reidel 1971b

Holzworth, R.H., Berthelier, J.-J., Cullers, D.K. Fahleson, U.V., Fälthammer, C.-G., Hudson, M.K., Jalonen, L., Kelley, M.C., Kellog, P.J., Tanskanen, P., Temerin, M., Mozer, F.S.: The large-scale ionospheric electric field: its variation with magnetic activity and relation to terrestrial kilometric radiation. J. Geophys. Res. **82**, 2735–2742, 1977

Horwitz, J.L., Doupnik, J.R., Banks, P.M.: Chatanika radar observations of the latitudinal distributions of auroral zone electric fields, conductivities, and currents. J. Geophys. Res. **83**, 1463–1481, 1978a

Horwitz, J.L., Doupnik, J.R., Banks, P.M., Kamide, Y., Akasofu, S.-I.: The latitudinal distributions of auroral zone electric fields and ground magnetic perturbations and their response to variations in the interplanetary magnetic field. J. Geophys. Res. **83**, 2071–2084, 1978b

Hughes, T.J., Rostoker, G.: Current flow in the magnetosphere and ionosphere during periods of moderate activity. J. Geophys. Res. **82**, 2271–2282, 1977

Hughes, T.J., Rostoker, G.: A comprehensive model current system for high-latitude magnetic activity – I. The steady state system. Geophys. J. R. Astron. Soc. **58**, 525–569, 1979

Iijima, T., Potemra, T.A.: The amplitude distribution of field-aligned currents at northern high latitudes observed by Triad. J. Geophys. Res. **81**, 2165–2174, 1976

Iijima, T., Potemra, T.A.: Large-scale characteristics of field-aligned currents associated with substorms. J. Geophys. Res. **83**, 599–615, 1978

Kamide, Y.: Recent progress in observational studies of electric fields and currents in the polar ionosphere: A review. Antarct. Rec. **63**, 61–231, 1979

Kamide, Y., Akasofu, S.-I.: The auroral electrojet and field-aligned current. Planet. Space Sci. **24**, 203–213, 1976

Kamide, Y., Akasofu, S.-I., Brekke, A.: Ionospheric currents obtained from the Chatanika radar and ground magnetic perturbations at the auroral latitude. Planet. Space Sci. **24**. 193–201, 1976a

Kamide, Y., Akasofu, S.-I., Rostoker, G.: Field-aligned currents and the auroral electrojet in the morning sector. J. Geophys. Res. **81**, 6141–6147, 1976b

Kamide, Y., Yasuhara, F., Akasofu, S.-I.: A model current system for the magnetospheric substorm. Planet. Space Sci. **24**, 215–222, 1976c

Kamide, Y., Brekke, A.: Auroral electrojet current density deduced from the Chatanika radar and from the Alaska meridian chain of magnetic observatories. J. Geophys. Res. **80**. 587–594, 1975

Kamide, Y., Brekke, A.: Altitude of the eastward and westward auroral electrojets. J. Geophys. Res. **82**, 2851–2853, 1977

Kamide, Y., Horowitz, J.L.: Chatanika radar observations of ionospheric and field-aligned currents. J. Geophys. Res. **83**. 1063–1070, 1978

Kamide, Y., Rostoker, G.: The spatial relationship of field-aligned currents and auroral electrojets to the distribution of nightside auroras. J. Geophys. Res. **82**, 5589–5608, 1977

Kelley, M.C., Starr, J.A., Mozer, F.S.: Relationship between magnetospheric electric fields and the motion of auroral forms. J. Geophys. Res. **76**, 5269–5277, 1971

Kertz, W.: Modelle für erdmagnetisch induzierte elektrische Ströme im Untergrund. Nachr. Akad. Wiss. Göttingen. Math. Phys. Kl. 101–110, 1954

Klumpar, D.M., Burrows, J.R., Wilson, M.D.: Simultaneous observations of field-aligned currents and particle fluxes in the post-midnight sector. Geophys. Res. Lett. **3**, 395–398. 1976

Küppers, F., Untiedt, J., Baumjohann, W., Lange, K., Jones. A.G.: A two-dimensional magnetometer array for ground-based observations of auroral zone electric currents during the International Magnetospheric Study (IMS). J. Geophys. **46**, 429–450, 1979

Lui, A.T.Y., Venkatesan, D., Anger, C.D., Akasofu, S.-I., Heikkila, W.J., Winningham, J.D., Burrows, J.R.: Simultaneous

observations of particle precipitations and auroral emissions by the Isis 2 satellite in the 19–24 MLT sector. J. Geophys. Res. **82**, 2210–2226, 1977

Mallinckrodt, A.J., Carlson, C.W.: Relations between transverse electric fields and the field-aligned currents. J. Geophys. Res. **83**, 1426–1432, 1978

Maynard, N.C.: Electric field measurements across the Harang discontinuity. J. Geophys. Res. **79**, 4620–4631, 1974

McDiarmid, I.B., Burrows, J.R., Budzinski, E.E.: Average characteristics of magnetospheric electrons (150 eV to 200 eV) at 1400 km. J. Geophys. Res. **80**, 73–79, 1975

Mende, S.B., Eather, R.H.: Monochromatic all-sky-observations and auroral precipitation patterns. J. Geophys. Res. **81**, 3771–3780, 1976

Mersmann, U., Baumjohann, W., Küppers, F., Lange, K.: Analysis of an eastward electrojet by means of upward continuation of ground-based magnetometer data. J. Geophys. **45**, 281–298, 1979

Mozer, F.S., Lucht, P.: The average auroral zone electric field. J. Geophys. Res. **79**, 1001–1006, 1974

Rostoker, G., Armstrong, J.C., Zmuda, A.J.: Field-aligned current flow associated with intrusion of the substorm-intensified westward electrojet into the evening sector. J. Geophys. Res. **80**, 3571–3579, 1975

Rostoker, G., Boström, R.: A mechanism for driving the gross Birkeland current configuration in the auroral oval. J. Geophys. Res. **81**, 235–244, 1976

Rostoker, G., Hughes, T.J.: A comprehensive model current system for high-latitude magnetic activity – II. The substorm component. Geophys. J. R. Astron. Soc. **58**, 571–581, 1979

Sesiano, J., Cloutier, P.A.: Measurements of field-aligned currents in a multiple auroral arc system. J. Geophys. Res. **81**, 116–122, 1976

Siebert, M., Kertz, W.: Zur Zerlegung eines lokalen erdmagnetischen Feldes in äußeren und inneren Anteil. Nachr. Akad. Wiss. Göttingen, Math. Phys. Kl. 87–112, 1957

Sugiura, M., Potemra, T.A.: Net field-aligned currents observed by Triad. J. Geophys. Res. **81**, 2155–2164, 1976

Vestine, E.H., Chapman, S.: The electric current-system of geomagnetic disturbance. Terr. Magn. Atmos. Electr. **43**, 351–382, 1938

Weaver, J.T.: On the separation of local geomagnetic fields into external and internal parts. Z. Geophys. **30**, 29–36, 1964

Wedde, T., Doupnik, J.R., Banks, P.M.: Chatanika observations of the latitudinal structure of electric fields and particle precipitation on November 21, 1975. J. Geophys. Res. **82**, 2743–2751, 1977

Yasuhara, F., Kamide, Y., Akasofu, S.-I.: Field-aligned and ionospheric currents. Planet. Space Sci. **23**, 1355–1368, 1975

Zmuda, A.J., Armstrong, J.C.: The dirunal flow pattern of field-aligned currents. J. Geophys. Res. **79**, 4611–4619, 1974

Received November 20, 1979; Revised Version January 22, 1980